ACADEMIC PRESS

Biochemical and Biophysical Research Communications 293 (2002) 566–571

BBRC

www.academicpress.com

Structural basis for inhibition of cyclin-dependent kinase 9 by flavopiridol

Walter Filgueira de Azevedo Jr.,[a,b,*] Fernanda Canduri,[a,b] and Nelson José Freitas da Silveira[a]

[a] *Departamento de Física, IBILCE, UNESP, São José do Rio Preto, SP 15054-000, Brazil*
[b] *Center for Applied Toxinology, Instituto Butantan Av. Vital Brasil, 1500, São Paulo, SP 05503-900, Brazil*

Received 26 March 2002

Abstract

Flavopiridol has been shown to potently inhibit CDK1 and 2 (cyclin-dependent kinases 1 and 2) and most recently it has been found that it also inhibits CDK9. The complex CDK9–cyclin T1 controls the elongation phase of transcription by RNA polymerase II. The present work describes a molecular model for the binary complex CDK9–flavopiridol. This structural model indicates that the inhibitor strongly binds to the ATP-binding pocket of CDK9 and the structural comparison of the complex CDK2–flavopiridol correlates the structural differences with differences in inhibition of these CDKs by flavopiridol. This structure opens the possibility of testing new inhibitor families, in addition to new substituents for the already known leading structures such as flavones and adenine derivatives.

Keywords: CDK; Flavopiridol; Bioinformatics; Structure; Drug design

Cell cycle progression is tightly controlled by the activity of cyclin-dependent kinases (CDKs) [1]. CDKs are inactive as monomers and activation requires binding to cyclins, a diverse family of proteins whose levels oscillate during the cell cycle, and phosphorylation by CDK-activating kinase (CAK) on a specific threonine residue [2]. In addition to the positive regulatory role of cyclins and CAK, many negative regulatory proteins (CDK inhibitors, CKIs) have been discovered [3]. Since deregulation of cyclins and/or alteration or absence of CKIs has been associated with many cancers, there is strong interest in chemical inhibitors of CDKs that could play an important role in the discovery of new family of antitumor agents [4]. CDKs also play a role in apoptosis (CDK2), in neuronal cells (CDK5), and in the control of transcription (CDK7, 8, 9) [5,6].

Flavopiridol is a CDK inhibitor, that is, in clinical trials cancer treatment because of its antiproliferative properties. It is a potential anticancer therapeutic agent currently being tested in phase I and II clinical trials. Treatment with flavopiridol resulted in blocking cell cycle progression, promoting differentiation, and inducing apoptosis in various types of cancerous cells [7]. A structure of CDK2 complexed with dechloflavopiridol revealed that the drug blocks in the ATP binding site [4], which helps to explain why inhibition of CDK2 is competitive with ATP.

Two previous studies demonstrated the effect of flavopiridol on transcription. Mammalian cells treated with this compound showed a decreased transcription of the gene encoding cyclin D1 [8] and high levels of flavopiridol affected levels of 63 different mRNAs in *Saccharomyces cerevisiae* [9]. The transcriptional inhibition observed in these studies could have been direct or a consequence of altered progression through the cell cycle. Furthermore, it has been shown that the binary complex CDK9–Cyclin T1 is potently inhibited by flavopiridol [5]. These results demonstrated that flavopiridol inhibited the complex CDK9–Cyclin T1 causing inhibition of transcription. The properties of the flavopiridol toward CDK9–Cyclin T1 complex suggest that the inhibitor should be examined as a potential HIV-1 therapy [5].

* Corresponding author. Fax: +1-55-17-221-2247.
E-mail address: walterfa@df.ibilce.unsep.br (W. Filgueira de Azevedo Jr.).

0006-291X/02/$ - see front matter
PII: S0006-291X(02)00266-8

This article describes the modeling of the human CDK9 complexed with flavopiridol inhibitor. The investigation was made to gain further insight into the structural basis for chemical inhibition of CDK9 by flavopiridol, which is the most effective CDK9 inhibitor described so far.

Methods

Molecular modeling. Homology modeling is usually the method of choice when there is a clear relationship of homology between the sequence of a target protein and at least one known structure. This computational technique is based on the assumption that the tertiary structures of two proteins will be similar if their sequences are related and it is the approach most likely to give accurate results [10]. There are two main approaches to homology modeling: (1) fragment-based comparative modeling [11,12] and (2) restrain-based modeling [13]. For modeling of the CDK9–flavopiridol complex we used the second approach. Model building of CDK9–flavopiridol was carried out using the program MODELLER [13]. MODELLER is an implementation of an automated approach to comparative modeling by satisfaction of spatial restraints [14–16]. The modeling procedure begins with an alignment of the sequence to be modeled (target) with related known three-dimensional structures (templates). This alignment is usually the input to the program. The output is a three-dimensional model for the target sequence containing all mainchain and sidechain non-hydrogen atoms.

Since there is no three-dimensional structure available for a CDK2–flavopiridol complex a model was built based on the atomic coordinates of CDK2–dechloroflavopridol complex, which was solved by cryocrystallographic methods [4]. The flavopiridol coordinates taken from the complex Glycogen Phosphorylase–flavopiridol (Access code: 1C8K) [17] were superposed to CDK2–dechloroflavopiridol [4] in order to obtain the CDK2–flavopiridol structure. The atomic coordinates for CDK2–flavopiridol were used as the starting model for modeling of the CDK9–flavopridol complex. The alignment of CDK2 (template) and CDK9 (target) is shown in Fig. 1. Fifteen residues from the N-terminal and 45 residues from the C-terminus were removed from the CDK9 model, since there is no good template for these fragments. Next, the spatial restraints and CHARMM energy terms enforcing proper stereochemistry [18] were combined into an objective function. Finally, the model is obtained by optimizing the objective function in Cartesian space. The optimization is carried out by the use of the variable target function method [19] employing methods of conjugate gradients and molecular dynamics with simulated annealing. Several slightly different models can be calculated by varying the initial structure. The final model is select based on stereochemical quality. All optimization processes were performed on SGI Octane, R12000.

Analysis of the model. The overall stereochemical quality of the final model for CDK9–Flavopiridol was assessed by the program PROCHECK [20]. Atomic models were superposed using the program LSQKAB from CCP4 [21]. The cutoff for hydrogen bonds and salt bridges was 3.9 Å. The contact surfaces for the binary complexes were calculated using AREAIMOL and RESAREA [21].

Results and discussion

Quality of the model

Ramachandran diagram ϕ–ψ plots for the binary complex of CDK9:Flavopiridol and for 10 crystallographic CDK2 structures solved to a resolution better than 2.1 Å were generated (figures not shown). The Ramachandran plot for the 10 CDK2 structures was used to compare the overall stereochemical quality of CDK9 model against CDK2 structures solved by biocrystallography. Analysis of the Ramachandran plot of the CDK9 model shows that 78.4% of the residues lies in the most favorable regions and the remaining 21.6% in the additional allowed regions. The same analysis for 10 crystallographic CDK2 structures presents almost 100 % of the residues in the most favorable and additional allowed regions, with one exception. The overall rating for the model is slightly worse than that obtained for the 10 structures of CDK2.

Overall description

The model of the kinase in the complex CDK9: Flavopiridol is folded into the typical bilobal structure, with the smaller N-terminal lobe consisting predominantly of a β-sheet structure and the larger C-terminal

```
                    15                  30                  45                  60                  75
CDK2 MENFQKVEKIGEGTYGVVYKARNKLTGEVVALKKIRLDTETEGVPSTAIREISLLKELNHPNIVKLLDVIHTEN--------KLYLVFEF     82
CDK9 VSKYEKLAKIGQGTFGEVFKARHRKTGQKVALKKVLMENEKEGFPITALREIKILQLLKHENVVNLIEICRTKASPYNRCKGSIYLVFDF     90
          *  *** ** * * ***   **  *****     * ** * ** ***  *  * * * * *     *            **** *

                   105                 120                 135                 150                 165
CDK2 LHQDLKKFMDASALTGIPLPLIKSYLFQLLQGLAFCHSHRVLHRDLKPQNLLINTEGAIKLADFGLARAFGVPVRT----YTHEVVTLWY    168
CDK9 CEHDLAGLLSN-VLVKFTLSEIKRVMQMLLNGLYYIHRNKILHRDMKAANVLITRDGVLKLADFGLARAFSLAKNSQPNRYTNRVVTLWY    179
        **        *    *  **     ** **   *    **** *  * **   *  ***********          **  ******

                   195                 210                 225                 240                 255
CDK2 RAPEILLGCKYYSTAVDIWSLGCIFAEMVTRRALFPGDSEIDQLFRIFRTLGTPDEVVWPGVTSMPDYKP-SFPKWARQDFSKVVPPLDE    257
CDK9 RPPELLLGERDYGPPIDLWGAGCIMAEMWTRSPIMQGNTEQHQLALISQLCGSITPEVWPNVDNYELYEKLELVKGQKRKVKDRLKAYVR    269
     * ** ***   *    * *  *** *** **     *  *  **  *    *     *** *     *      *

                   285                 300
CDK2 D--GRSLLSQMLHYDPNKRISAKAALAHPFFQDVTKPVPHLRL    298
CDK9 DPYALDLIDKLLVLDPAQRIDSDDALNHDFFWSDPMPSDLKGM    312
     *     *    *  **  **    ** * **     *
```

Fig. 1. Sequence alignment of human CDK2 and CDK9. There are 40.4% of identity between CDK2 and CDK9 sequences, in the modelled region. The multiple alignment was performed with the program CLUSTAL V [34].

lobe consisting primarily of α-helices. The N-terminal lobe of CDK9 consists of a sheet of five antiparallel-strands (β1–β5) and a single large helix (α1). The C-terminal lobe contains a pseudo-4-helical bundle (α2,3,4,6), a small β-ribbon (β6–β8), and two additional helices (α5,7). Fig. 2 shows a schematic drawing of the complex CDK9–Flavopridol. The flavopiridol molecule is found in the cleft between the two lobes. The core (the β-sheet and the helical bundle) of the CDK9 structure is very similar to that of the CDK2 [22]. The conserved core consists of a small lobe associated primarily with ATP binding and a large lobe associated with peptide binding and catalysis. In CDK9, the residues 93–95 present a β-sheet, while in CDK2 this region (residues 85–87) is in random coil. Most of the residues conserved throughout the protein kinase family cluster around the active cleft [23].

Molecular fork

The participation of a molecular fork composed of C=O group on Glu 81, N–H group, and C=O group in Leu 83 in hydrogen bonds between CDK2 and inhibitor has been observed in several CDK2–Inhibitor structures. This molecular fork, composed of two hydrogen bond acceptors (C=O) and one hydrogen bond donor (N–H), allows for a wide range of different molecular geometries to dock onto the ATP binding pocket, such as: olomoucine, isopentenyladenine, roscovitine [24,25], staurosporine [26], purvalanols [9], indirubins [27], hymenialdisine [28], and NU2058 [29]. Table 1 shows the hydrogen bond distances between the molecular fork of CDK2 and different inhibitors. All these inhibitors have pairs of hydrogen bond partners that show complementarity to the molecular fork on CDK2, most of them involving at least two hydrogen bonds with the molecular fork. The relative orientation of the inhibitor in the binding pocket of CDK2 locates one hydrogen bond donor close to C=O on Glu 81 and/or Leu 83, and an acceptor close to N–H on Leu 83. Such a simple paradigm is conserved in all CDK2–Inhibitor complex structures solved so far. In the CDK9–Flavopiridol model this molecular fork is composed of C=O on Asp 89, N–H and C=O on Cys 91 and participates in the hydrogen bonds between CDK9 and flavopiridol.

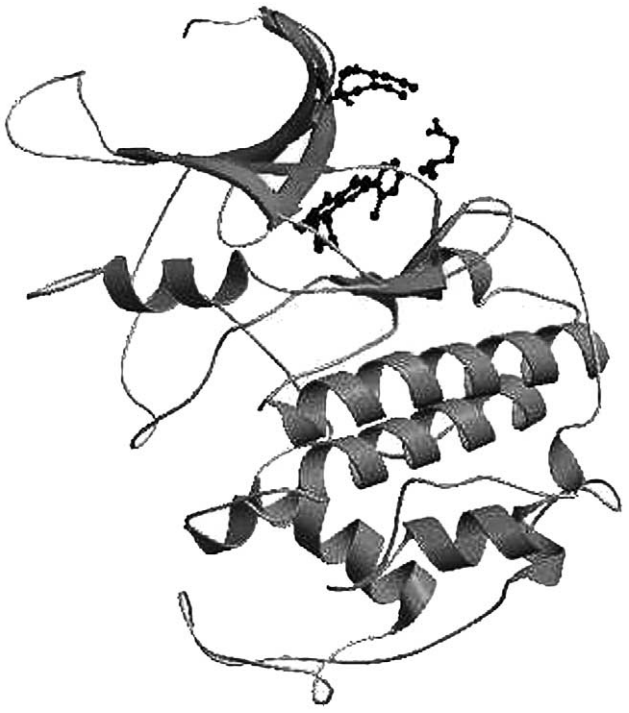

Fig. 2. Ribbon diagram of the human CDK9 generated by Molscript [35] and Raster3D [36] showing the residues Lys 20, Lys 29, and Glu 92.

Interactions of flavopirdol with CDK9

The specificity and affinity between enzyme and its inhibitor depend on directional hydrogen bonds and ionic interactions, as well as on shape complementarity of the contact surfaces of both partners [25,30,31]. It was observed a total of 6 hydrogen bonds between CDK9 and flavopiridol, in binary model, involving the residues Lys 33, Asp 89, Cys 91, Asn 139, and Asp 152. For the

Table 1
Hydrogen bonds between the molecular fork of CDK2 and inhibitor

Inhibitor	Distance between inhibitor and C=O on Glu 81 (Å)	Distance between inhibitor and N–H on Leu 83 (Å)	Distance between inhibitor and C=O on Leu 83 (Å)
Staurosporine	2.75	2.63	NO
Purvalanol B	3.73	3.18	2.54
Hymenialdisine	2.76	2.74	3.17
NU2058	2.57	3.11	2.34
NU6027	2.84	2.97	2.49
U55	NO	3.30	2.74
PKFO 49-38	2.71	3.13	3.27
Dechloroflavopiridol	2.86	2.91	NO
Roscovitine	NO	3.38	2.82
Olomoucine	NO	2.94	2.65
Isopentenyladenine	NO	3.39	NO
Indirubins	3.04	2.72	3.10

NO: Not observed.

Table 2
Hydrogen bonds between CDK2:Flavopiridol

Hydrogen bonds between active site and inhibitor			Distance (Å)
Flavopiridol	CDK2		
O5	Glu 81	O	2.88
O4	Leu 83	N	2.73
N1	Asp 152	OD2	3.60
O3	Asp 152	OD2	3.19
O3	Lys 33	NZ	3.03

Table 3
Hydrogen bonds between CDK9:flavopiridol

Hydrogen bonds between active site and inhibitor			Distance (Å)
Flavopiridol	CDK9		
N1	Asp 152	$O^{\delta 2}$	3.79
N1	Asn 139	$O^{\delta 1}$	3.90
O3	Lys 33	NZ	3.41
O7	Lys 33	NZ	3.87
O5	Asp 89	O	2.77
O4	Cys 91	N	2.75

CDK2:Flavopiridol model it was observed 5 hydrogen bonds involving the residues Lys 33, Glu 81, Leu 83, and Asp 152. Tables 2 and 3 show the intermolecular hydrogen bonds for both structures. As observed for the crystallographic structure of dechloroflavopiridol bound to CDK2 [4], the region of CDK9 occupied by the chlorophenyl ring of flavopiridol is pointing away from the ATP-binding pocket, and partially exposed to solvent.

Superposition of the complexes of flavopiridol with CDK2 and CDK9 is shown on Fig. 3A. The benzopyran ring of flavopiridol occupies the same region in both complexes. This region is the same occupied by the purine ring of ATP in the CDK2:ATP complex [32]. Superposition of the CDK2:ATP onto CDK9:flavopiridol structure indicates that the two ring systems overlap approximately in the same plane, but the benzopyran is rotated about 52.5° relative to the adenine in ATP, measured as the angle between the carbon–carbon bonds joining the two cycles in benzopyran and adenine rings, respectively. Fig. 3B shows the ATP-binding pocket for the complexes CDK2–ATP and CDK9–Flavopiridol.

Two strong salt bridges are observed between Glu 92–Lys 20 and Glu 92–Lys 29 in the CDK9–Flavopiridol structure, theses salt bridges involve residues from two different lobes of the CDK9 structure and they are not conserved on the CDK2 structures, Lys 20 and 29 in the N-terminal lobe and Glu 92 in the C-terminal lobe. This strong eletrostatic interaction brings the two lobes of CDK9 closer, which increases the contact area between enzyme and inhibitor. Fig. 2 shows the position of the salt bridges on the CDK9 structure. Furthermore the side chains of Glu 92, Lys 20, and Lys 29 brings the phenyl of Phe 90 to a position deeper in the binding pocket, which also contributed to increase the contact area between flavopiridol and CDK9.

The electrostatic potential surface of the CDK2–Flavopiridol and the model of CDK9 complexed with same inhibitor were calculated with GRASP [33] (figure not shown). The analysis of the charge distribution of the binding pockets indicates the presence of some charge complementarity between inhibitor and enzyme, nevertheless most of the binding pocket is hydrophobic in both structures.

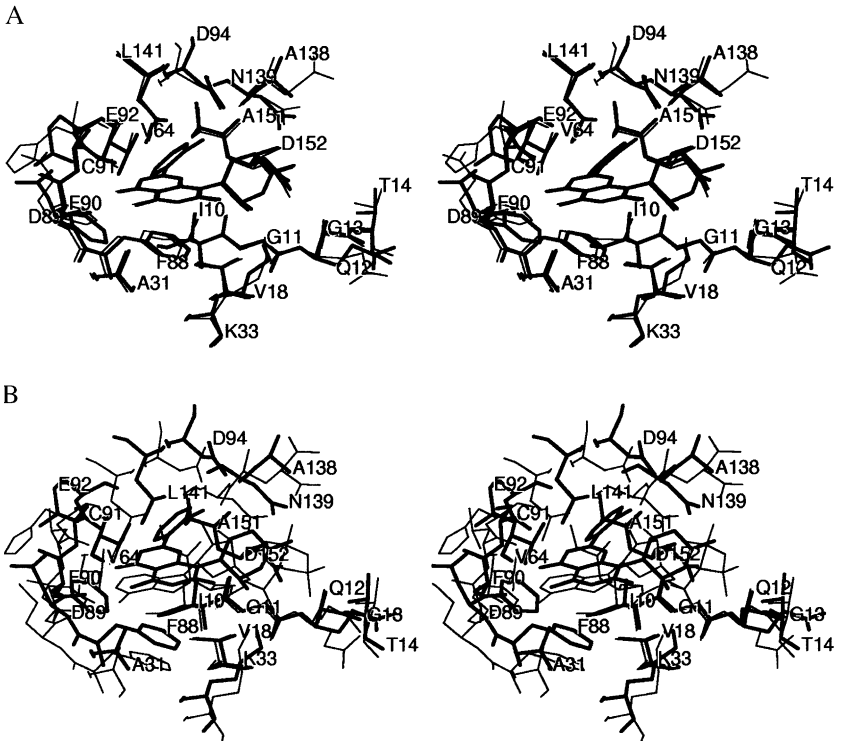

Fig. 3. (a) Superimposed binding pockets of CDK9:Flavopiridol complex (thick line) and CDK2:Flavopiridol complex (thin line). (b) Superimposed binding pockets of CDK9:Flavopiridol complex (thick line) and CDK2:ATP complex (thin line).

Table 4
Summary of structural results for CDK2 and CDK9

	CDK2	CDK9
Contact area for the complexes with flavopiridol (Å^2)	320	332
Number of the hydrogen bonds between protein and inhibitor	5	6
IC50 (μM)	0.4	0.2

Especially interesting is the previous functional study of inhibition of CDK9 by flavopiridol, which indicated lack of competition with ATP, suggesting the presence of at least one additional binding site [5]. A close inspection of the CDK9 model did not reveal the presence of any additional binding pockets. The CDK9: Flavopiridol model clearly reveals a very tight binding of the inhibitor to the enzyme which may essentially inactivates the enzyme, in such scenery a competitive kinetic mechanism is possible.

The contact areas for the complexes of CDK2 and CDK9 with flavopiridol are 320 and 332 Å^2 respectively, which may partially explain the lower IC50 value observed for CDK9. In addition, the CDK9–Flavopiridol complex shows a higher number of intermolecular hydrogen bonds, which also indicates that flavopiridol has higher affinity for CDK9. Table 4 summarizes the some structural results and IC50 for CDK2 and CDK9 structures. The overall structure of the complex indicates that the flavopiridol is tightly bound to the ATP-binding pocket and since no further binding sites were identified in the CDK9 structure we have strong structural evidence that flavopiridol is a competitive inhibitor with ATP.

The simple paradigm of the molecular fork, also identified in CDK9 structure, suggests that CDK9 may also be strongly inhibited by other CDK2 inhibitors, such as roscovitine, olomoucine, and staurosporine. Further inhibition experiments may confirm this prediction. Fig. 4 shows a schematic diagram for this molecular fork.

It has been observed that the complex CDK9–Cyclin T1 is a key factor in HIV-1 infection and flavopiridol blocks HIV-1 propagation in cultured cells. Furthermore, it has been suggested that flavopiridol should be evaluated as a potential AIDS therapy [5] and the CDK9 structural model can be used for designing new active CDK9 inhibitors.

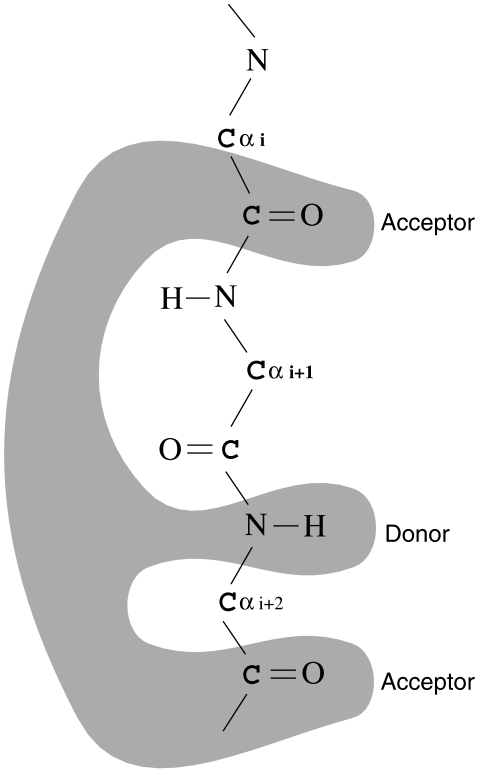

Fig. 4. Schematic diagram of the molecular fork. Residues from i to $i+2$ are Glu 81, Phe 82, Leu 83, and Asp 89, Phe 90, Cys 91 for CDK2 and CDK9, respectively.

Acknowledgments

We thank Andressa Salbé dos Santos Oliveira for English revision. This work was supported by grants from FAPESP (SMOLBNet), CNPq, CAPES and Fundo Bunka de Pesquisa (Banco Sumitomo). WFAJr. is a researcher for the Brazilian Council for Scientific and Technological Development (CNPq, 300851/98-7).

References

[1] C. Norbury, P. Nurse, Animal cell cycles and their control, Annu. Rev. Biochem. 61 (1992) 441–470.
[2] D. Desai, Y. Gu, D.O. Morgan, Activation of human cyclin-dependent kinases in vitro, Mol. Biol. Cell 3 (1992) 571–582.
[3] H.E. Richardson, C.S. Stueland, J. Thomas, P. Russel, S.I. Reed, Human cDNAs encoding homologs of the small p34Cdc28/Cdc2-associated protein of *Saccharomyces cerevisiae* and *Schizosaccharomyces pombe*, Genes Dev. 4 (1990) 1332–1344.
[4] W.F. deAzevedo Jr., H.J. Mueller-Dieckmann, U. Schulze-Gahmen, P.J. Worland, E. Sausville, S.-H. Kim, Structural basis for specificity and potency of a flavonoid inhibitor of human CDK2 acell cycle kinase, Proc. Natl. Acad. Sci. USA 93 (7) (1996) 2735–2740.
[5] S.H. Chao, K. Fujinaga, J.E. Marion, R. Taube, E.A. Sausville, A.M. Senderowicz, B.M. Peterlin, D.H.J. Price, Flavopiridol inhibits P-TEFb and blocks HIV-1 replication, J. Biol. Chem. 275 (37) (2000) 28345–28348.
[6] N. Gray, L. Detivaud, C. Doerig, L. Meijer, Curr, ATP-site directed inhibitors of cyclin-dependent kinases, Curr. Med. Chem. 6 (9) (1999) 859–875.
[7] A.M. Senderowicz, E.A. Sausville, Preclinical and clinical development of cyclin-dependent kinase modulators, J. Natl. Cancer Inst. 92 (5) (2000) 376–387.
[8] B.A. Carlson, T. Lahusen, S. Singh, A. Loaiza-Perez, P.J. Worland, R. Pestell, C. Albanese, E.A. Sausville, A.M. Senderowicz, Down regulation of cyclin D1 by transcriptional

repression in MCF-7 human breast carcinoma cells induced by flavopiridol, Cancer Res. 59 (1999) 4634–4641.
[9] N.S. Gray, L. Wodicka, A.M. Thunniessen, T.C. Norman, S. Kwon, F.H. Espinoza, D.O. Morgan, G. Barnes, S. LeClerc, L. Meijer, S.H. Kim, D.J. Lockhart, P.G. Schultz, Exploiting chemical libraries, structure, and genomics in the search for kinase inhibitors, Science 281 (1998) 533–538.
[10] R.T. Kroemer, S.W. Doughty, A.J. Robinson, W.G. Richards, Prediction of the three-dimensional structure of human interleukin-7 by homology modeling, Protein Eng. 9 (6) (1996) 493–498.
[11] T.L. Blundell, B.L. Sibanda, M.J. Sternberg, J.M. Thornton, Knowledge-based prediction of protein structures and the design of novel molecules, Nature 326 (6111) (1987) 347–352.
[12] T.L. Blundell, D. Carney, S. Gardner, F. Hayes, B. Howlin, T. Hubbard, J. Overington, D.A. Singh, B.L. Sibanda, M. Sutcliffe, 18th Krebs, Hans Lecture—knowledge-based protein modeling and design, Eur. J. Biochem. 172 (3) (1988) 513–520.
[13] A. Sali, T.L. Blundell, Comparative protein modelling by satisfaction of spatial restraints, J. Mol. Biol. 234 (1993) 779–815.
[14] A. Sali, J.P. Overington, Derivation of rules for comparative protein modeling from a database of protein structure alignments, Protein Sci. 3 (9) (1994) 1582–1596.
[15] A. Sali, L. Potterton, F. Yuan, H. Vlijmen, M. Karplus, Evaluation of comparative protein modeling by MODELLER, Proteins 23 (3) (1995) 318–326.
[16] A. Sali, Modeling mutations and homologous proteins, Curr. Opin. Biotechnol. 6 (4) (1995) 437–451.
[17] N.G. Oikonomakos, J.B. Schnier, S.E. Zographos, V.T. Skamnaki, K.E. Tsitsanou, L.N. Johnson, Flavopiridol inhibits glycogen phosphorylase by binding at the inhibitor site, J. Biol. Chem. 275 (44) (2000) 34566–34573.
[18] B.R. Brooks, R.E. Bruccoleri, B.D. Olafson, D.J. States, S. Swaminathan, M. Karplus, CHARMM: a program for macromolecular energy minimization and dynamics calculations, J. Comp. Chem. 4 (1983) 187–217.
[19] W. Braun, N. Go, Calculation of protein conformations by proton-proton distance constraints. A new efficient algorithm, J. Mol. Biol. 186 (3) (1985) 611–626.
[20] R.A. Laskowski, M.W. MacArthur, D.K. Smith, D.T. Jones, E.G. Hutchinson, A.L. Morris, D. Naylor, D.S. Moss, J.M. Thorton, PROCHECK v.3.0—Program to Check the Stereochemistry Quality of Protein Structures—Operating Instructions, 1994.
[21] Collaborative Computational Project No. 4., 1994. The CCP4 suite: programs for protein crystallography. Acta Crystallogr. D 50, 760–763.
[22] H.L. DeBondt, J. Rosenblatt, J. Jancarik, H.D. Jones, D.O. Morgan, S.-H. Kim, Crystal structural of cyclin-dependent kinase 2, Nature (London) 363 (1993) 595–602.
[23] S. Serota, E. Radsio-Andzelm, Three protein kinase structures define a common motif, Structure 2 (1994) 345–355.
[24] U. Schultze-Gahmen, J. Brandsen, H.D. Jones, D.O. Morgan, I. Meijer, J. Vesely, Multiple modes of ligand recognition: crystal structures of cyclin-dependent protein kinase 2 in the complex with ATP and two inhibitors, olomoucine and isopentenyladenine, Proteins 22 (1995) 378–391.
[25] W.F. DeAzevedo Jr., S. Leclerc, L. Meijer, L. Havlicek, M. Strnad, S.-H. Kim, Inhibition of cyclin-dependent kinases bypurine analogues: crystal structure of human CDK2 complexed with roscovitine, Eur. J. Biochem. 243 (1997) 518–526.
[26] A.M. Lawrie, M.E. Noble, P. Tunnah, N.R. Brown, L.N. Johnson, J.A. Endicott, Protein kinase inhibition by staurosporine revealed in details of the molecular interaction with CDK2, Nat. Struct. Biol. 4 (1997) 796.
[27] R. Hoessel, S. Leclerc, J.A. Endicott, M.E. Nobel, A. Lawrie, P. Tunnah, M. Leost, E. Damiens, D. Marie, D. Marko, E. Niederberger, W. Tang, G. Eisenbrand, L. Meijer, Indirubin, the active constituent of a Chinese antileukaemia medicine, inhibits cyclin-dependent kinases, Nat. Cell Biol. 1 (1) (1999) 60–67.
[28] L. Meijer, A. Borgne, O. Mulner, J.P. Chong, J.J. Blow, N. Inagaki, Biochemical and cellular effects of roscovitine, apatent and selective inhibitor of the cyclin-dependent kinases CDK2 and CDK5, Eur. J. Biochem. 243 (1997) 527–536.
[29] C.E. Arris, F.T. Boyle, A.H. Calvert, N.J. Curtin, J.A. Endicott, E.F. Garman, A.E. Gibson, B.T. Golding, S. Grant, R.J. Griffin, P. Jewsbury, L.N. Johnson, A.M. Lawrie, D.R. Newell, M.E. Noble, E.A. Sausville, R. Schultz, W. Yu, Identification of novel purine and pyrimidine cyclin-dependent kinase inhibitors with distinct molecular interactions and tumor cell growth inhibition profiles, J. Med. Chem. 43 (15) (2000) 2797–2804.
[30] F. Canduri, L.G.V.L. Teodoro, C.C.B. Lorenzi, V. Hial, R.A.S. Gomes, J. Ruggiero Neto, W.F. de Azevedo Jr., Crystal structure of human uropepsin at 2.45 Å resolution, Acta Crystallogr. D 57 (2001) 1560–1570.
[31] W.F. DeAzevedo Jr., F. Canduri, V. Fadel, L.G.V.L. Teodoro, V. Hial, R.A.S. Gomes, Molecular model for the binary complex of uropepsin and pepstatin, Biochem. Biophys. Res. Commun. 287 (1) (2001) 277–281.
[32] S.-H. Kim, U. Schulze-Gahmen, J. Brandsen, W.F. de Azevedo Jr., Structural basis for chemical inhibitor of CDK2, Prog. Cell Cycle Res. 2 (1996) 137–145.
[33] A. Nicholls, K.A. Sharp, B. Honig, Protein folding and association: insights from the interfacial and thermodynamic properties of hydrocarbons, Proteins 11 (4) (1991) 281–296.
[34] D.G. Higgins, A.J. Bleasby, R. Fuchs, CLUSTAL V: improved software for multiple sequence alignment, Comput. Appl. Biosci. 8 (2) (1992) 189–191.
[35] P. Kraulis, MOLSCRIPT: a program to produce both detailed and schematic plots of proteins, J. Appl. Cryst. 24 (1991) 946–950.
[36] E.A. Merritt, D.J. Bacon, Raster3D: photorealistic molecular graphics, Methods Enzimol. 277 (1997) 505–524.